Acta Pharmaceutica Sinica B 2024;14(8):3576−3590

Chinese Pharmaceutical Association
Institute of Materia Medica, Chinese Academy of Medical Sciences

Acta Pharmaceutica Sinica B

www.elsevier.com/locate/apsb
www.sciencedirect.com

ORIGINAL ARTICLE

Mechanical regulation of lipid and sugar absorption by Piezo1 in enterocytes

Tian Tao[a,b], Qing Shu[a], Yawen Zhao[a], Wenying Guo[a], Jinting Wang[a], Yuhao Shi[a], Shiqi Jia[b], Hening Zhai[c], Hui Chen[d], Cunchuan Wang[b,*], Geyang Xu[a,e,*]

[a]*Department of Physiology, School of Medicine, Jinan University, Guangzhou 510632, China*
[b]*Department of Metabolic and Bariatric Surgery, the First Affiliated Hospital of Jinan University, Guangzhou 510630, China*
[c]*Endoscopy Center, the First Affiliated Hospital of Jinan University, Guangzhou 510630, China*
[d]*Biotherapy Center; Cell-gene Therapy Translational Medicine Research Center, the Third Affiliated Hospital, Sun Yat-sen University, Guangzhou 510630, China*
[e]*Key Laboratory of Viral Pathogenesis & Infection Prevention and Control (Jinan University), Ministry of Education, Guangzhou 510632, China*

Received 25 November 2023; received in revised form 22 March 2024; accepted 27 March 2024

KEY WORDS

Piezo1;
DGAT2;
SGLT1;
Lipid metabolism;
Obesity;
Mechanical sensing;
Intestinal lipid absorption;
Intestinal glucose absorption

Abstract Obesity is primarily caused by excessive intake as well as absorption of sugar and lipid. Postprandial surge in distention pressure and intestinal motility accelerates the absorption of nutrients. The response of intestinal epithelial cells to mechanical stimulation is not fully understood. Piezo1, a mechanosensitive ion channel, is widely expressed throughout the digestive tract. However, its function in intestinal nutrient absorption is not yet clear. In our study, excessive lipid deposition was observed in the duodenum of obese patients, while duodenal Piezo1−CaMKK2−AMPKα was decreased when compared to normal-weight individuals. Under high-fat diet condition, the *Piezo1*^{iKO} mice exhibited abnormally elevated sugar and lipid absorption as well as severe lipid deposition in the duodenum and liver. These phenotypes were mainly caused by the inhibition of duodenal CaMKK2−AMPKα and the upregulation of SGLT1 and DGAT2. In contrast, Yoda1, a Piezo1 agonist, was found to reduce intestinal lipid absorption in diet induced obese mice. Overexpression of Piezo1, stretch and Yoda1 inhibited lipid accumulation and the expression of DGAT2 and SGLT1, whereas knockdown of Piezo1 stimulated lipid accumulation and DGAT2 in Caco-2 cells. Our study reveals a previously unexplored mechanical regulation of nutrient absorption in intestinal epithelial cells, which may shed new light on the therapy of obesity.

*Corresponding authors.
E-mail addresses: xugeyangliang@163.com (Geyang Xu), twcc@jnu.edu.cn (Cunchuan Wang).

Peer review under the responsibility of Chinese Pharmaceutical Association and Institute of Materia Medica, Chinese Academy of Medical Sciences.

https://doi.org/10.1016/j.apsb.2024.04.016

1. Introduction

Obesity is emerging as a significant global public health concern. The excessive intake and absorption of nutrients are increasingly recognized as contributing factors to the growing epidemics of obesity[1,2]. It is reported that obese patients tend to absorb the nutrients more efficiently and promptly, especially in their upper small intestines[3]. The duodenum and jejunum are the major sites for the digestion and absorption of dietary sugar and fat[4]. After being decomposed by digestive enzymes, the monosaccharides are transported into intestinal epithelial cells followed by entrance into the blood circulation. Sodium-dependent glucose cotransporter 1 (SGLT1) and glucose transporter 2 (GLUT2) are the most important glucose transporters in this procedure[5]. More importantly, accelerated intestinal lipid absorption is another primary impetus of obesity[6]. Lipid absorption is a complex multi-step process. Dietary triacylglycerols (TAGs) are emulsified and hydrolyzed into free fatty acids and monoacylglycerols in the lumen of the intestine. Fatty acids are taken up from the gut lumen into enterocytes by either passive transport or active transport mediated *via* CD36 and/or fatty acid transport protein 4 (FATP4)[7,8]. Subsequently, the digested products are transported to the endoplasmic reticulum (ER), where TAG is then re-synthesized. The monoacylglycerol (MAG) pathway and the glycerol 3-phosphate pathway are major pathways to re-synthesize triacylglycerol (TAG), and the MAG pathway accounts for 75%−80% of TAG synthesis[9-11]. In the MAG pathway, monoacylglycerol acyltransferase (MGAT) catalyzes the MAG to diacylglycerol (DAG), diacylglycerol acyltransferase (DGAT) catalyzes the DAG to triacylglycerol (TAG)[12,13]. Catalyzing DAG to generate TAG is a major rate-limiting step. The TAGs are then used for chylomicron packaging and enter the lymphatics to eventually re-enter the blood circulation[14]. During these processes, APOB is an essential protein required for chylomicron packaging in the small intestine[15]. Previous studies illustrated that the development of obesity is associated with the abnormal expression of the absorption-associated proteins such as CD36, DGAT1, DGAT2, MGAT2, APOB and SGLT1. Pharmacotherapy targeting absorption-associated proteins could be used to treat obesity and its associated complications[16−22].

After primary digestion in the stomach, chyme enters into duodenum. It is notable that intestinal epithelial cells receive the mechanical stimulation when the chyme passing through the intestine, including stretching, pressure and shear force[23]. The mechanosensing in enterocytes and its role in nutrient absorption is still unexplored. Piezo1 is a mechanosensitive ion channel that converts mechanical force into electrical and chemical signals *via* transmembrane calcium influx[24]. Piezo1 is widely expressed in nonsensory tissues including the lung, endothelial cells, erythrocytes, urinary bladder and kidney[25]. It plays crucial roles in various physiological processes such as stabilizing lung endothelial barriers[26], regulating blood pressure[27], maintaining vascular integrity[28], as well as contributing to erythrocyte volume homeostasis[29] and mechanosensory transduction in the urinary system[30]. In the gastrointestinal epithelium, Piezo1 channels act as pressure sensors to regulate cell proliferation and migration, mucosal barrier function and intestinal motility[31−33]. Thus we assume that Piezo1-mediated mechanosensing in enterocytes regulates intestinal nutrient absorption.

In the present study, intestinal lipid accumulation was observed in obese patients, which was associated with a decrement of Piezo1. To better understand the role of Piezo1 in enterocytes, we created a mouse model with specific deletion of Piezo1 in intestinal epithelial cells (*Piezo1*^{iKO}). We observed a slight increase in lipid accumulation in the duodenum and liver under normal chow diet conditions. After fed with high fat-diet, *Piezo1*^{iKO} mice displayed over-absorption of fat and sugar, impaired glucose homoeostasis and severe lipid deposits in multiple organs. Pharmacological, mechanical and genetic manipulations of Piezo1 regulated the expression of DGAT2 and SGLT1 as well as sugar and lipid accumulation in Caco-2 cells. Mechanistically, Piezo1 regulates DGAT2 and SGLT1 *via* Ca^{2+}/CaMKK2/AMPKα pathway. In sum, current study reveals that Piezo1 functions as a suppressor of sugar and lipid absorption in intestinal epithelium cells. We propose that mechanoperception in the enterocytes plays a crucial role in nutrient absorption, and targeting intestinal Piezo1 may offer a promising approach for the therapy of obesity and diabetes.

2. Methods and materials

2.1. Materials

Yoda1, olive oil and glucose were purchased from Sigma−Aldrich (St. Louis, MO, USA). GsMTx4 was purchased from Alomone Labs Ltd. (Jerusalem, Israel). STO-609 was obtained from Selleck Chemicals (Houston, TX, USA). Anti-SGLT1 (1:1000 dilution), and anti-β-actin (1:10,000 dilution) antibodies were purchased from Abcam (Cambridge, MA, USA). Anti-PIEZO1 (1:1000 dilution), anti-DGAT2 (1:1000 dilution), anti-CD36 (1:1000 dilution), anti-APOB (1:1000 dilution), anti-CaMKK2 (1:1000 dilution) antibodies were obtained from Affinity Biosciences (Cincinnati, OH, USA). Anti-PGC1α (1:1000 dilution) and anti-ACADL (1:1000 dilution) antibodies were purchased from Proteintech (Chicago, IL, USA). Anti-AMPKα (1:1000 dilution) and anti-Phospho-AMPKα (Thr172) (1:1000 dilution) antibodies were purchased from Cell Signaling Technology (Danvers, MA, USA).

2.2. Animals

The mice used in this study were housed in specific pathogen-free conditions and all animal experiments complied with the relevant ethical regulations. All animal protocols were approved by the Animal Care and Use Committee of Jinan University.

Piezo1$^{flox/flox}$ mice and *Villin-cre* mice were obtained from Jackson Laboratory (Bar Harbor, ME). To generate intestinal epithelium cell-specific Piezo1 deletion mice (*Piezo1*^{iKO}), the *Piezo1*$^{flox/flox}$ mice were crossed with the *Villin-Cre* mice. PCR is used to identify the genotype of mice during the subsequent

mating and breeding process. The primers required for mouse genotyping are shown in the Supporting Information Table S1.

2.3. Yoda1 treatment

After 8 weeks of HFD feeding, Yoda1 was administrated to C57BL/6 mice intraperitoneally (i.p.) at a dose of 80 μg/kg once daily for a week. Body weight was monitored daily.

2.4. Food and water intake detection

The food and water consumption were measured using the metabolic cages with feeding/drinking analysis (Cat. No. 41853, Ugo basile, Comerio, Italy). Mice were singly housed and acclimatized in metabolic chambers for three days before data collection. Mice had free access to food and water. Each mouse was continuously monitored for food and water intake. Data was recorded and analyzed by software/interface package 41850-010 which includes EXPEDATA (data analysis) and METASCREEN (data acquisition) software and IM-2 Interface Module. Additionally, the urine and feces were collected daily.

2.5. Xylose or oil gavage experiments

The *Piezo1*^{iKO} and control mice were fasted overnight and received the administration of either 1 g/kg or 10 μL/g body weight of D-xylose or olive oil *via* gavage, respectively. Blood samples were collected from the tail vein before oral administration and at different time points thereafter. The plasma levels of D-xylose were measured using commercial kits (Solaibao, Beijing, China) in accordance with the provided instructions. Plasma TAG and FFA were determined using commercial kits (Boxbio, Shanghai, China) according to the instructions.

2.6. IPGTT and ITT

For the IPGTT, the *Piezo1*^{iKO} and control mice were fasted overnight and then injected intraperitoneally with glucose (1.5 g/kg). The Insulin Tolerance Test (ITT) was performed on mice that were fasted for 4 h and then received an intraperitoneal injection of insulin (0.5 IU/kg for NCD mice, 1 IU/kg for HFD mice). Blood sample was collected from the tail vein at various time points (0, 15, 30, 60, 90, 120 min) for glucose determination using the Accu-Chek Performa glucometer (Roche).

2.7. Biochemical analysis

FFA and TAG levels in blood, liver, duodenum and feces were measured and determined using commercial kits (Boxbio, Shanghai, China) according to the instructions. Biochemical analysis was performed as described previously[34].

2.8. H&E staining

Paraffin-embedded sections were cut and stained with hematoxylin and eosin. Image acquisition was performed with Lecia microscope (Leica, Germany).

2.9. Oil-red O staining

The liver and duodenum were fixed in 4% paraformaldehyde and embedded in O.C.T. compound for histological analysis. To perform Oil-red O staining, 10-μm-thick slices of the tissues were cut and stained with Oil-red O. Hematoxylin was used to stain the nucleus, and the red lipid droplets were observed microscopically.

2.10. Immunofluorescent staining

The sections underwent standard dewaxing, followed by antigen retrieval treatment. Primary antibodies for PIEZO1 (1:400 dilution), DGAT2 (1:100 dilution), and SGLT1 (1:100 dilution) were incubated overnight at 4 °C with the sections. After washing with PBS, fluorescein-conjugated secondary antibodies were added, and the sections were counterstained with DAPI. The images were captured using a Lecia SP8 microscope (Leica, Germany).

2.11. Cell culture and transfection

The human Caco-2 cells were obtained from the American Type Culture Collection (ATCC, Manassas, VA, USA) and were maintained in DMEM containing 10% fetal bovine serum (FBS) at 37 °C in a 5% CO_2 humidified atmosphere.

For stable knockdown of Piezo1 in Caco-2 cells, Firstly, shRNA sequences for human Piezo1 interference were cloned in to pLKO.1 vector. psPAX2, pMD2G and pLKO.1 or pLKO.1-shPiezo1 plasmids (siPiezo1: CCCTGTGCATTGATTATCCT) were co-transfected into 293T cells for 48 h to produce lentiviral supernatants. After collecting and filtering, the lentiviral supernatants were added to the culture medium of Caco-2 cells for 24 h. After that, the Caco-2 cells were subjected to 5 μg/mL puromycin selection for 48 h.

2.12. Real-time PCR

Total RNA was extracted using Trizol reagent (Takara, Shiga, Japan) and reversely transcribed to cDNA. qPCR was performed using SYBR Green Master Mix according to the manufacturer's instructions. Primers are listed in Supporting Information Table S2.

2.13. Western blotting

Western blot analysis was performed as described previously[35,36]. Briefly, the proteins were separated by SDS-PAGE and detected with specific antibodies.

2.14. Luciferase reporter assay

Caco-2 cells were co-transfected with Dgat2 luciferase reporter (generously gifted by Prof. Baojian Wu, Guangzhou University of Chinese Medicine, Guangzhou, China) and pRL-TK plasmids. Cells were then transfected with GFP or Piezo1 constructs using transfection reagent, or treated with 10 μmol/L of STO-609 for 24 h. Cell lysates were analyzed for luciferase activity with the dual-luciferase reporter assay system according to the manufacturer's instructions.

2.15. Collection of human intestine samples

Five normal-weight individuals and five obese individuals were enrolled in the study. All participants had not taken any drugs one week before biopsy collection. Participation in this study was voluntary and written informed consent was obtained from each participant. All protocols were approved by the Institutional Review Board of Jinan University (Guangzhou, China).

2.16. Detection of glucose uptake with fluorescent D-glucose analog (2-NBDG) in Caco-2 cells

Glucose uptake was assessed using the glucose analogue 2-NBDG (MedChem Express, Monmouth Junction, NJ, USA), which was conducted in the Caco-2 monolayer model. Caco-2 cells and Piezo1 knockdown Caco-2 cells were treated with Yoda1 (5 μmol/L) for 24 h, after which the cells medium was replaced with PBS buffer containing 2-NBDG (100 μmol/L), then incubated at 37 °C for 30 min. The wells were then washed three times with PBS to eliminate excess 2-NBDG. Subsequently, 2-NBDG imaging was performed using a 488 nm laser, and pictures were taken with an inverted fluorescence microscope.

2.17. Cell mechanical stretching assay

Caco-2 cells were cultured in 0.1% gelatin-coated silicone elastic chambers, then chambers were placed on manual retractors and subjected to mechanical stretch to 120% of their original length.

2.18. Calcium imaging

Caco-2 cells were seeded onto confocal dishes at optimal densities and cultured for 24 h. Subsequently, the cells were incubated with the calcium fluorescent probe fluo-4 AM (1 μmol/L) (Thermo Fisher Scientific, Waltham, MA, USA) for 1 h at 37 °C. After that, cells were treated with Yoda1 and/or GsMTx4. Intracellular calcium ions were measured at room temperature using a laser confocal microscope. The change in fluorescent signal was presented as $\Delta F/F_0$ and plotted against time.

2.19. Whole-cell patch-clamp recording

Caco-2 cells were cultured on sterile glass coverslips and subsequently utilized for patch clamping experiments. Patch pipettes made of borosilicate glass were pulled using a micropipette puller and then fire-polished to achieve a resistance of 3−5 MΩ. The inward current of the Caco-2 cells was amplified, filtered, and recorded using the EPC10 USB patch-clamp amplifier (HEKA, Germany) along with PatchMaster software for data acquisition and analysis. The electrode solution contained 138 mmol/L KCl, 10 mmol/L NaCl, 1 mmol/L $MgCl_2$, 10 mmol/L glucose and 10 mmol/L HEPES (pH 7.4). The extracellular solution contained 130 mmol/L NaCl, 5 mmol/L KCl, 1 mmol/L $MgCl_2$, 2.5 mmol/L $CaCl_2$, 10 mmol/L glucose, 20 mmol/L HEPES (pH7.4).

2.20. Statistical analyses

All data were expressed as mean ± standard error of mean (SEM). Statistical differences were evaluated by one-way ANOVA, repeated ANOVA or Student's *t*-test. $P < 0.05$ was considered significant. $^*P < 0.05$, $^{**}P < 0.01$, $^{***}P < 0.001$. Randomization and blinding manner were used whenever possible. The sample size in animal studies was determined on the basis of previous experience with similar animal studies.

3. Results

3.1. Expression of Piezo1 and nutrient absorption-related proteins in human and mouse duodenal biopsies

The human duodenal biopsies from normal-weight and obese individuals were collected to determine the duodenal sugar and lipid metabolism. Impaired metabolic parameters, including plasma glucose and lipid, were observed in obese patients (Fig. 1A−D). Greater villi length and severe lipid deposition were detected in the duodenum of the obese individuals (Fig. 1E and F). Meanwhile, immunofluorescent staining confirmed that PIEZO1 was highly expressed in the intestinal epithelium of normal-weight participants while it was decreased in the intestinal epithelium of obese subjects (Fig. 1G). In contrast to PIEZO1, DGAT2 was highly expressed in the duodenum of obese individuals but not in lean controls (Fig. 1H). mRNA and protein levels of Piezo1 were significantly lower in duodenum of obese participants than that in controls, while the expression levels of CD36, DGAT2 and SGLT1 were increased in the duodenum of obese individuals (Fig. 1I−K). Piezo1 is considered as a calcium channel[24]. Calmodulin serves as an intracellular Ca^{2+}-receptor and mediates the regulation of downstream processes and pathways by Ca^{2+}. Calcium/calmodulin-dependent protein kinase 2 (CaMKK2) is a serine/threonine-protein kinase that belongs to the Ca^{2+}/calmodulin-dependent protein kinase subfamily[37]. CaMKK2 is the main calcium/calmodulin dependent protein kinase involved in the regulation of metabolic homeostasis[38]. Previous studies have illustrated that CaMKK2 regulates glucose and lipid metabolism *via* AMPK[38]. In current study, decreased duodenal CaMKK2−AMPKα signaling pathway was observed in obese individuals when compared with lean controls (Fig. 1J and K).

Similarly, the expression of Piezo1 in the duodenum of NCD and HFD mice was detected using RT-PCR and Western blot. Both mRNA and protein levels of Piezo1 were found to be decreased in HFD mice compared to NCD mice (Fig. 1L−N). Moreover, refeeding after fasting significantly stimulated the expression of Piezo1 in the duodenum of male C57/BL6 mice. (Supporting Information Fig. S1).

3.2. Deficiency of intestinal Piezo1 promotes obesity upon high-fat-diet feeding

In order to observe the role of Piezo1 in enterocytes, *Villin-Cre* mice were crossed to $Piezo1^{fl/fl}$ to generate mice with enterocytes (ECs)-specific deletion of Piezo1($Piezo1^{iKO}$) (Fig. 2A). $Piezo1^{iKO}$ mice were identified by PCR genotyping of genomic DNA from tail biopsies (Fig. 2B). No statistical difference was observed in body weight, liver weight, epididymal fat weight and glucose metabolism between $Piezo1^{iKO}$ and $Piezo1^{fl/fl}$ mice under normal chow diet (NCD) (Fig. 2C−G). Conversely, the $Piezo1^{iKO}$ mice exhibited significant increases in body weight, liver weight, and epididymal fat weight when they were exposed to high-fat diet (HFD) (Fig. 2C−E). Additionally, the $Piezo1^{iKO}$ mice exhibited glucose intolerance and insulin resistance under the HFD (Fig. 2H and I). No differences in food intake (both NCD and HFD) and water intake were observed between $Piezo1^{iKO}$ and $Piezo1^{fl/fl}$ mice (Fig. 2J−M).

Under a normal chow diet condition, the size of adipocytes was increased in $Piezo1^{iKO}$ mice, while the liver HE staining showed

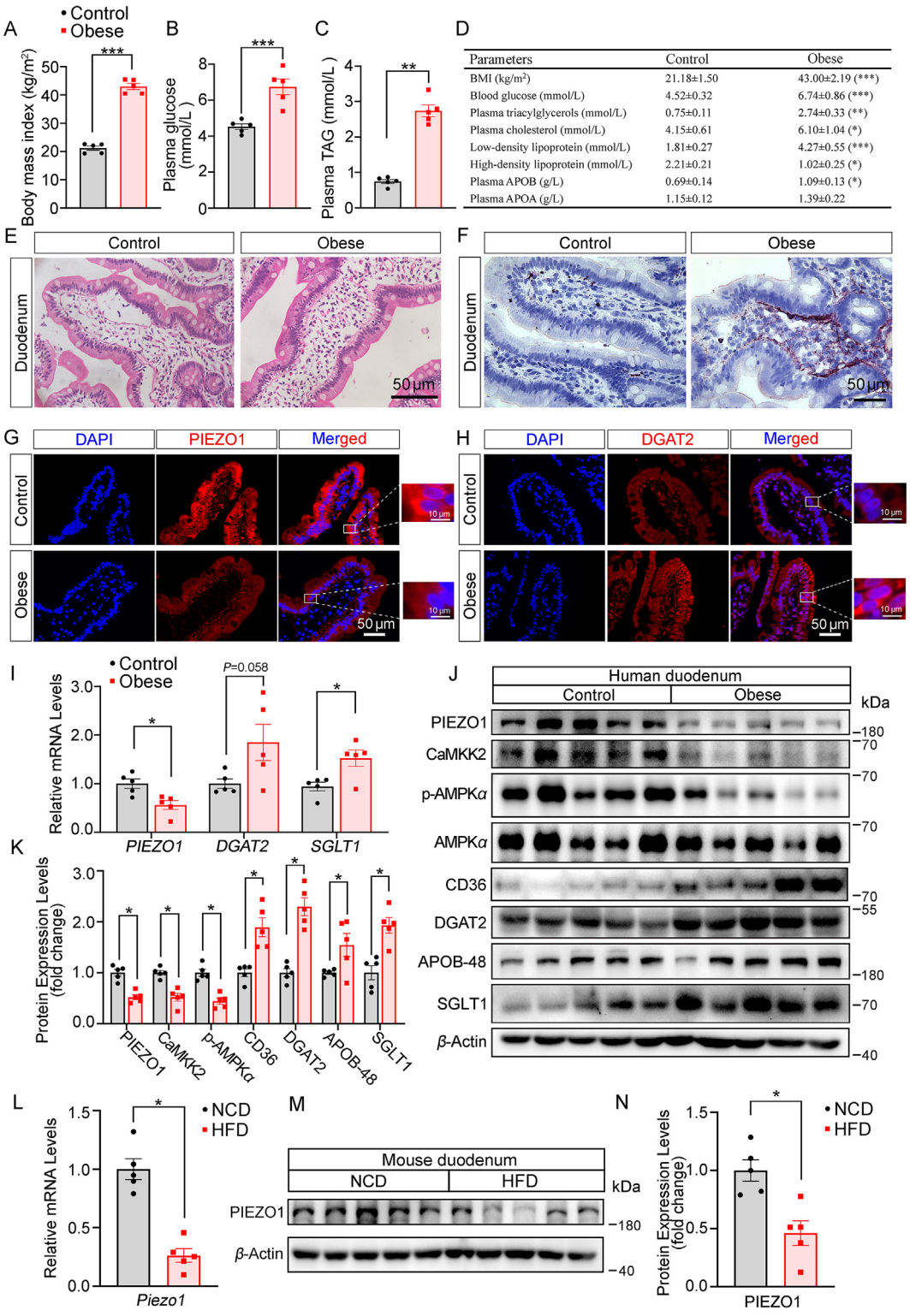

Figure 1 Expression of Piezo1 and nutrient absorption-related proteins in human duodenums. (A–C) Body mass index (BMI), fasting blood glucose, plasma triacylglycerol of normal weight subjects and obese participants. (D) Biochemical indicator levels related to lipid metabolism were summarized. (E, F) Representative HE staining of duodenum and oil red O staining of duodenum in normal weight subjects (Control) and obese participants (Obese). (G, H) The immunofluorescent staining of PIEZO1 and DGAT2 (red immunofluorescence) in the duodenum of normal-weight individuals and obese participants. (I) The mRNA levels of *PIEZO1*, *DGAT2* and *SGLT1*. (J, K) Representative Western blots are shown for PIEZO1, CaMKK2, p-AMPKα, AMPKα, CD36, DGAT2, APOB-48 and SGLT1 in the duodenum of normal weight individuals and obese subjects and the quantification of protein levels. (L) The mRNA levels of *Piezo1* in the duodenum of NCD and HFD mouse. (M, N) Representative Western blots and quantified results are shown for PIEZO1. Results are expressed as mean ± SEM, $n = 5$; $^{*}P < 0.05$, $^{**}P < 0.01$, $^{***}P < 0.001$.

no appreciable change. Increased hepatic lipid accumulation was found in *Piezo1*^{iKO} mice under NCD according to the Oil-red O (ORO) staining. However, HFD-fed *Piezo1*^{iKO} mice demonstrated enlarged adipocytes in white adipose tissue (WAT) and severe lipid deposit in the liver (Fig. 2N−P).

3.3. Intestinal sugar and lipid absorption was increased in *Piezo1*^{iKO} mice upon high-fat-diet feeding

To further investigate the effect of intestinal epithelial cell-specific Piezo1 deletion on nutrient metabolism, we assayed the levels of blood, hepatic, and duodenal lipids. No significant differences were observed in circulating levels of TAG and the excretion of TAG. However, hepatic and duodenal lipid levels were increased in *Piezo1*^{iKO} mice under NCD (Fig. 3A−E). Additionally, levels of TAG in blood, liver, and duodenum were significantly elevated in *Piezo1*^{iKO} mice, while fecal lipid contents were reduced in *Piezo1*^{iKO} mice under high-fat diet conditions (Fig. 3A−E). According to D-xylose and olive oil gavage assays, increased absorption of sugar and lipid was observed in the *Piezo1*^{iKO} mice in both NCD- and HFD-feeding conditions (Fig. 3F−H). The HE staining results of duodenum indicated that, compared to the control mice, the villi of the *Piezo1*^{iKO} mice showed a more slender and elongated morphology, accompanied by a decrease in crypt depth (Fig. 3I). Furthermore, Oil-red O staining of the duodenum showed enhanced lipid accumulation in *Piezo1*^{iKO} mice in both NCD and HFD conditions (Fig. 3J).

3.4. Intestinal ablation of *Piezo1* up-regulates expression of *DGAT2* and *SGLT1* in the duodenum

The major genes and proteins responsible for sugar and lipid absorption processes were measured using RT-PCR and Western blot. The results indicated a reduction in the expression of Piezo1 in the duodenum of *Piezo1*^{iKO} mice (Fig. 4A and B). As expected, up-regulation of SGLT1 and DGAT2 in the duodenum of *Piezo1*^{iKO} mice was observed under both low- and high-fat diet conditions, which was associated with decreased duodenal CaMKK2−AMPKα (Fig. 4A and B).

However, the mRNA levels of fatty acid oxidation-related genes such as *Pgc1α*, *Pparα*, and *Acadl* were increased in *Piezo1*^{iKO} mice under NCD, while they were decreased under HFD (Fig. 4A). Furthermore, Western blot analysis revealed an up-regulation of PGC1α, and ACADL in the proximal intestine of *Piezo1*^{iKO} mice under NCD (Fig. 4B), while PGC1α and ACADL were decreased under HFD (Fig. 4B). Additionally, the staining results also revealed a notable increase in DGAT2 and SGLT1 levels in *Piezo1*^{iKO} mice when compared to controls under HFD (Fig. 4C and D).

3.5. Yoda1 inhibits lipid absorption in high-fat diet-induced obese mice

Yoda1, a specific agonist of Piezo1, was administered to further investigate the impact of Piezo1 on intestinal glucose and lipid metabolism in a high-fat diet-induced obese C57/BL6 mice. Treatment with Yoda1 resulted in a reduction in body weight gain (Fig. 5A). Yoda1-treated mice exhibited decreased levels of TAG and FFA in the proximal small intestine, along with increased fecal TAG and FFA levels. Treatment of Yoda1 also resulted in a decrease in plasma TAG levels (Fig. 5B−D). Oil-red O staining demonstrated that Yoda1 reduced the lipid accumulation in the duodenum (Fig. 5E). Furthermore, Yoda1 activated the CaMKK2−AMPKα signaling pathway and inhibited the expression levels of CD36, DGAT2, APOB, and SGLT1. It also increased the expression levels of PGC1α and ACADL. (Fig. 5F−H).

3.6. Pharmacological, mechanical and genetic activation of *Piezo1* inhibits lipid accumulation in Caco-2 cells

To further validate the role of Piezo1 in lipid metabolism *in vitro*, we examined the effect of manipulating Piezo1 in lipid metabolism on Caco-2 cells. Pharmacological activation of Piezo1 by Yoda1 triggered an inward current in Caco-2 cell recorded by whole cell patch-clamp, which could be inhibited by pre-incubation of GsMTx4 (Fig. 6A). The results of calcium imaging demonstrated Yoda1 also triggered an increase in intracellular Ca^{2+} level in Caco-2 cells. Pre-incubation of cells with GsMTx4 (0.1 μmol/L) for 30 min inhibited $[Ca^{2+}]_i$ increase (Fig. 6B). Yoda1 at the dose of 5 μmol/L activated CaMKK2−AMPKα signaling pathway and inhibited the expression levels of DGAT2 and SGLT1, consequently improving lipid accumulation within the Caco-2 cells in both presence and absence of oleic acid (Fig. 6C−F). Furthermore, as shown in Supporting Information Fig. S2, the effects of Yoda1 on CaMKK2−AMPKα signaling pathway and expression of DGAT2/SGLT1 were disappeared in Piezo1 knockdown Caco-2 cells.

To mimic the activation of Piezo1 by mechanical stretching, Caco-2 cells were grown on an elastic modulus were subjected to mechanical stretch, the results revealed that mechanical stretch inhibited DGAT2 and SGLT1 and activated CaMKK2−AMPKα signaling pathway in Caco-2 cells (Fig. 6G−I).

Furthermore, over-expression of Piezo1 alleviated lipid deposition within the Caco-2 cells, which was associated with the inhibition of CD36, DGAT2 and SGLT1 (Fig. 6J−M). A luciferase reporter assay indicated that Piezo1 could inhibit the promoter activity of DGAT2 (Fig. 6N).

3.7. Effects of inhibiting *Piezo1* or *CaMKK2* on the sugar and lipid metabolism in Caco-2 cells

To further investigate the role of Piezo1 in sugar and lipid metabolism *in vitro*, a stable knockdown of Piezo1 in Caco-2 cell line was constructed. Knockdown of Piezo1 up-regulated the protein levels of CD36, DGAT2, and SGLT1 in Caco-2 cells (Fig. 7A and B). Oil-red O staining demonstrated lipid accumulation was increased in Caco-2 cells with stable knockdown of Piezo1, especially in these cells treated with oleic acid (Fig. 7C). CaMKK2−AMPKα signaling pathway was inhibited in Piezo1-knockdown Caco-2 cells, Moreover, both mRNA and protein levels of DGAT2 and SGLT1 were found to be elevated, while the protein level of CD36 was also increased (Fig. 7D−F).

We conducted a glucose uptake experiment on Caco-2 cells using 2-NBDG, the results showed that knocking down of Piezo1 significantly increased the uptake of glucose analogs in Caco-2 cells. Treatment of Yoda1 reduced glucose uptake in Caco-2 cells, but this effect was disappeared when the Piezo1 was knockdown in Caco-2 cells (Fig. 7G).

Furthermore, STO-609, a specific inhibitor of CaMKK2, inhibited AMPKα phosphorylation while increased the expression levels of DGAT2 and SGLT1 in Caco-2 cells. STO-609 also stimulated the promoter activity of DGAT2 (Fig. 7H−K).

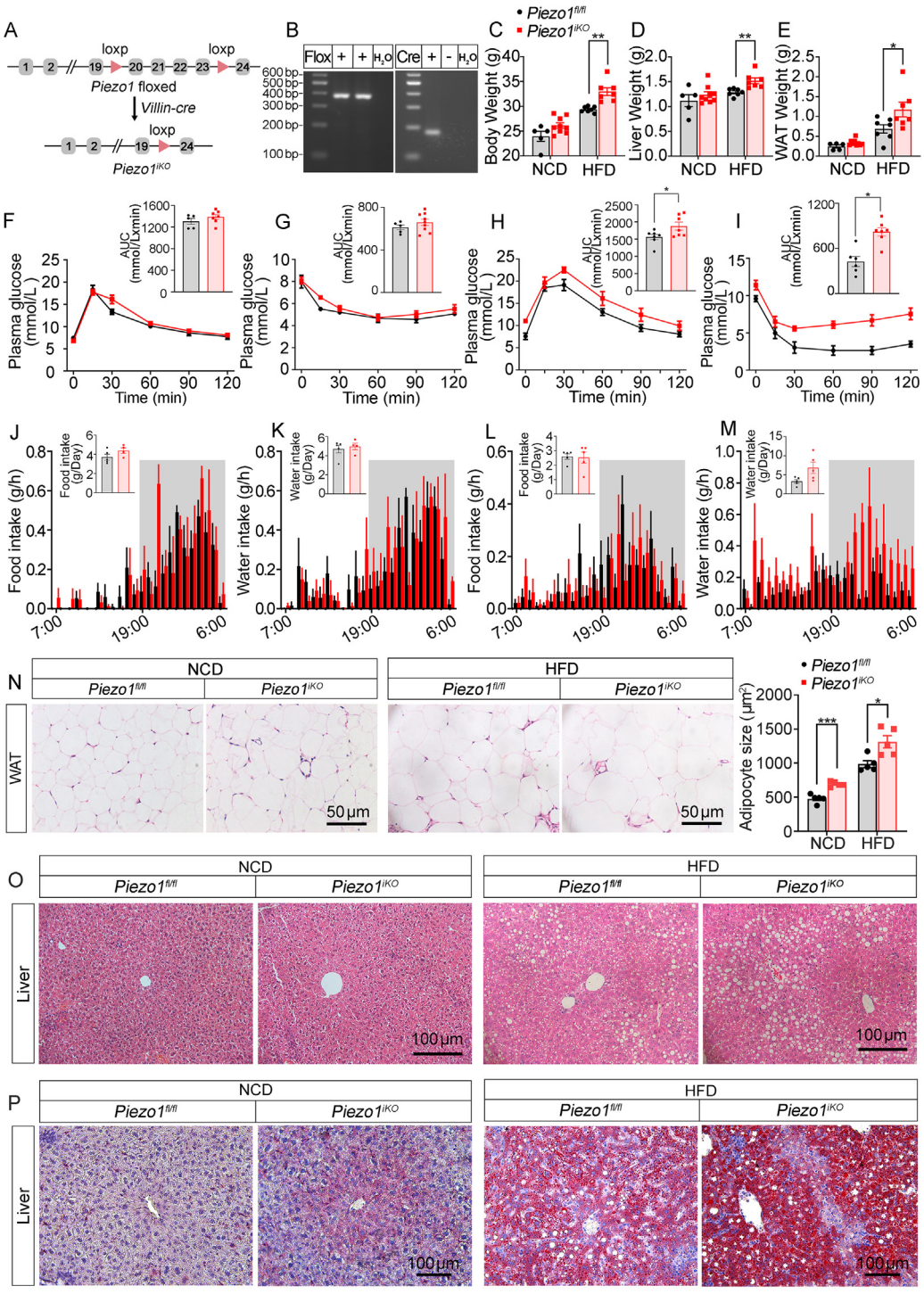

Figure 2 Deficiency of intestinal Piezo1 promotes obesity upon high-fat-diet feeding. (A) Strategy of the generation of enterocytes (ECs)-specific knockout mouse. (B) Genotyping PCR results. (C) Body weight, (D) liver weight and (E) fat weight of control and *Piezo1*^{iKO} mice fed with normal chow diet and high fat diet (n = 5−9/group). (F) IPGTT and the area under the curve (n = 5−7/group), (G) ITT and the area under the curve (n = 5−9/group) of mice fed with NCD. (H) IPGTT and the area under the curve (n = 7/group), (I) ITT and the area under the curve (n = 6 or 7/group) of mice fed with HFD. (J, K) Food intake and water intake of control and *Piezo1*^{iKO} mice under NCD (n = 4 or 5/group). (L, M) High-fat diet intake and water intake of control and *Piezo1*^{iKO} mice under HFD (n = 5/group). (N) Representative HE-stained images of white adipose tissue (WAT) (n = 5/group). (O, P) Representative HE staining images and Oil-Red O staining images of livers (n = 4 or 5/group). Results are expressed as mean ± SEM; $^{*}P < 0.05$, $^{**}P < 0.01$, $^{***}P < 0.001$.

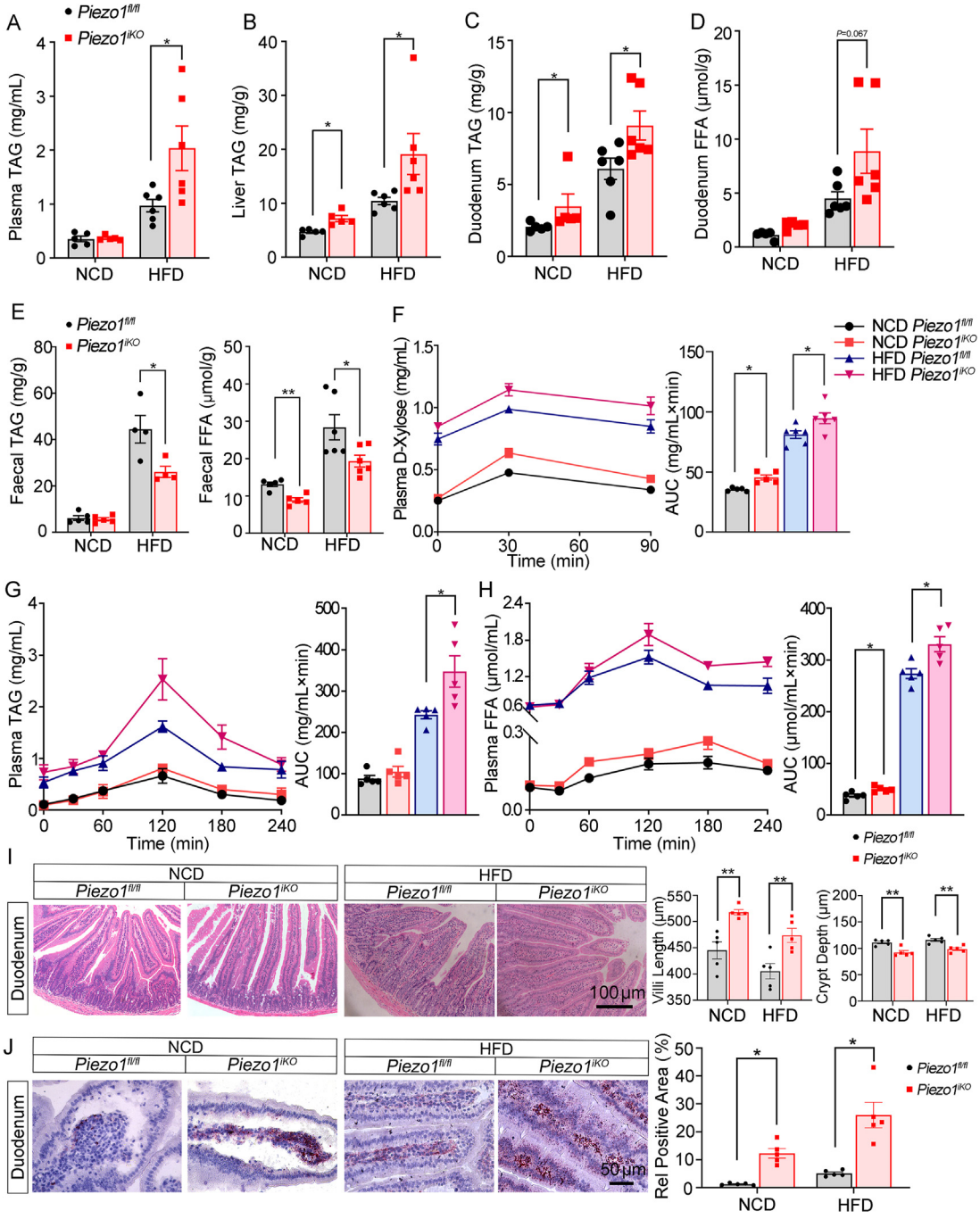

Figure 3 Intestinal sugar and lipid absorption were increased in *Piezo1*^{iKO} mice upon high-fat-diet feeding. (A) Plasma TAG levels in *Piezo1*$^{fl/fl}$ and *Piezo1*^{iKO} mice fed with NCD and HFD ($n = 5$ or 6). (B) Hepatic TAG levels ($n = 5$ or 6). (C) Duodenal TAG levels ($n = 5$ or 6). (D) Duodenal FFA levels in control and *Piezo1*^{iKO} mice ($n = 5$ or 6). (E) Fecal TAG and FFA levels ($n = 4$−6). (F) Plasma xylose levels in control and *Piezo1*^{iKO} mice after oral gavage of xylose ($n = 5$ or 6). (G) Plasma TAG and (H) FFA levels in control and *Piezo1*^{iKO} mice after oral gavage of olive oil (10 μL/g) ($n = 5$). (I) Representative HE staining of duodenum and quantification of villi length and crypt depth ($n = 5$). (J) Red O staining photos of duodenum and quantitation ($n = 5$). Results are expressed as mean ± SEM; $^{*}P < 0.05$, $^{**}P < 0.01$, $^{***}P < 0.001$.

4. Discussion

Dietary sugars and fats are major sources of energy for the body. Defects in the process of nutrient absorption can lead to malnutrition, while excessive nutrient intake and absorption contribute to obesity and metabolic disorders[39]. Gastric emptying rate[40], pH[41], gut microbiota[42], secretion of digestive juices[43], nutrient transporters[44], hormonal[45] and neural signals[46] are master regulators of nutrient absorption. Most carbohydrates in the chyme are digested by salivary and pancreatic amylases, which further broken down into monosaccharides. Monosaccharides are absorbed by carrier-mediated transport such as SGLT1 and GLUT2 across intestinal epithelial cells[5]. In morbid obesity, proximal intestine glucose absorption is accelerated and is associated with

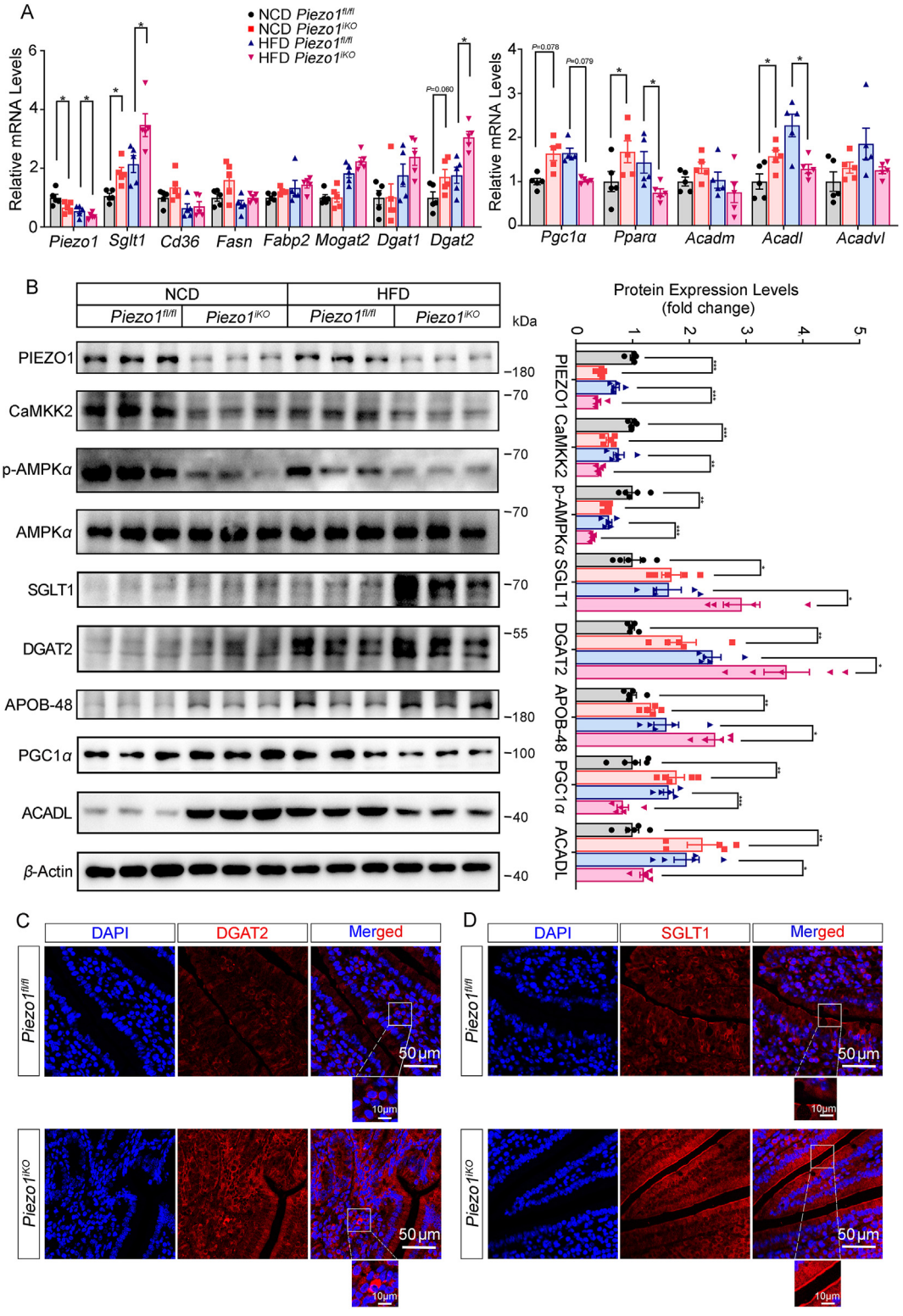

Figure 4 Expression of absorption-related proteins in *Piezo1*^{iKO} mice. (A) RT-PCR analysis of the major genes responsible for nutrient absorption and lipid metabolism in duodenum of the control and *Piezo1*^{iKO} mice fed with NCD and HFD (n = 5/group). (B) Representative Western blots for duodenal PIEZO1, CaMKK2, p-AMPKα, AMPKα, DGAT2, APOB-48, SGLT1, PGC1α, ACADL and β-actin (n = 5/group) and quantitative Western blot analysis (n = 5/group). (C, D) Representative duodenal images of immunofluorescence staining of DGAT2 and SGLT1 in HFD-fed mice. Results are expressed as mean ± SEM; $^{*}P < 0.05$, $^{**}P < 0.01$, $^{***}P < 0.001$.

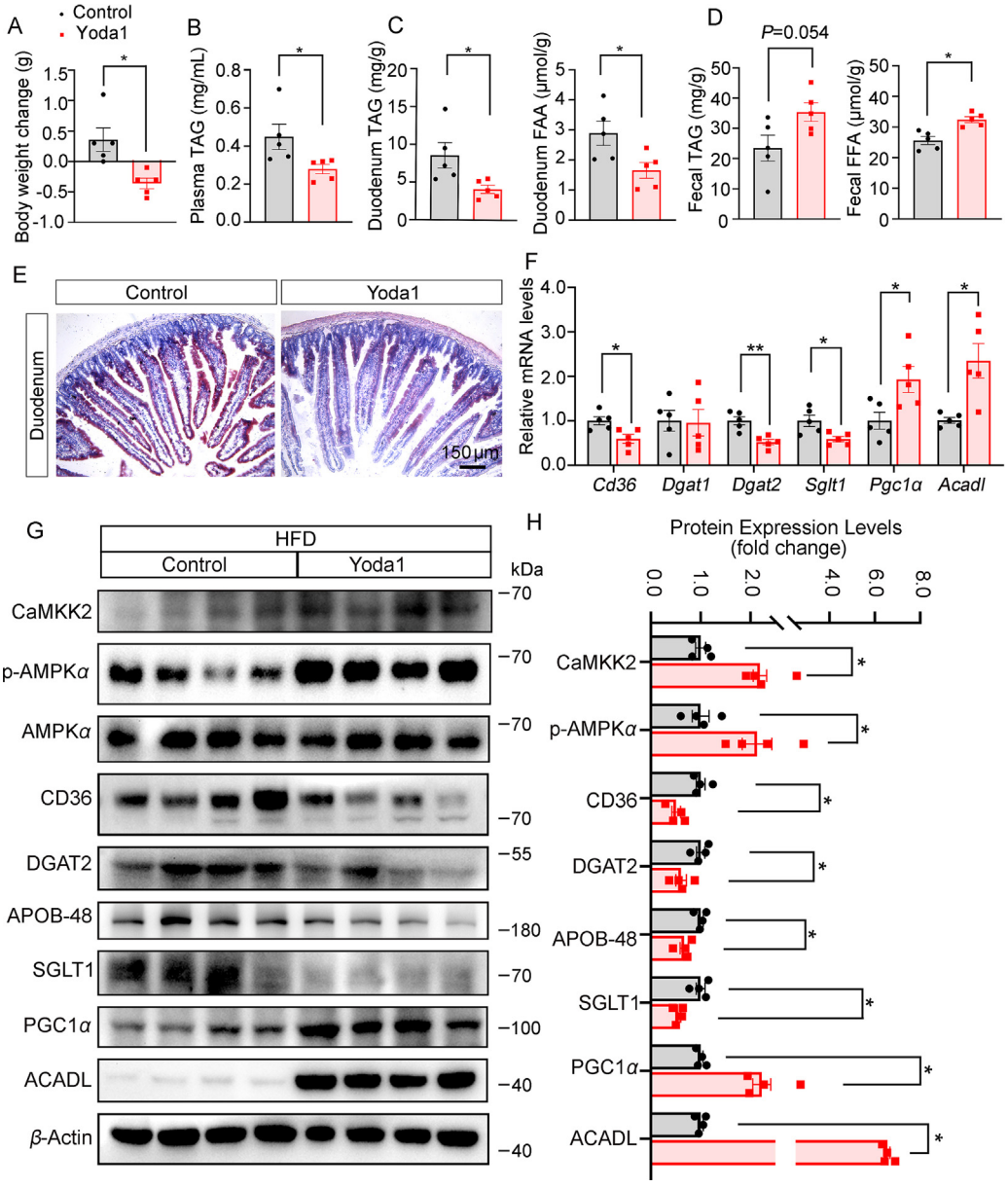

Figure 5 Yoda1 inhibits lipid absorption in high-fat diet-induced obese mice. (A) Body weight change of DIO mice infusion of vehicle or Yoda1 for 7 days (n = 5/group). (B) Plasma TAG levels (n = 5/group). (C) Duodenal TAG and FFA levels (n = 5/group). (D) Fecal TAG and FFA levels (n = 5/group). (E) Representative Red O staining images of duodenum. (F) *Cd36*, *Dgat1*, *Dgat2*, *Sglt1*, *Pgc1α*, *Acadl* mRNA levels (n = 5/group). (G) Representative Western blots for duodenal CaMKK2, p-AMPKα, AMPKα, CD36, DGAT2, APOB-48, SGLT1, PGC1α, ACADL and β-actin. (n = 4/group). (H) Quantitative Western blot analysis. Results are expressed as mean ± SEM; $^{*}P < 0.05$, $^{**}P < 0.01$, $^{***}P < 0.001$.

the amount of SGLT1[47]. In the current study, obese patients exhibited greater duodenal villus and elevated levels of blood glucose, which was accompanied by a similar change in levels of SGLT1. To further investigate the role of Piezo1 in enterocytes, we developed an intestinal epithelial cell-specific Piezo1 knockout mouse model utilizing Cre-loxP recombination system. The *Piezo1*^{iKO} mice under high-fat diet showed hyperglycemia and accelerated absorption of D-xylose, which were also associated with up-regulation of duodenal SGLT1. Over-expression of Piezo1 and stretch inhibited SGLT1 while knockdown of Piezo1 exerted the opposite effects in Caco-2 cells. Pharmacological activation of Piezo1 inhibited glucose uptake in Caco-2. These results suggest that Piezo1−SGLT1 is vital to the sugar absorption in the intestine.

Unlike sugar, the absorption of lipids is more complicated including fatty acid uptake, TAG resynthesis, chylomicron assembly, trafficking, and secretion processes in enterocytes[48]. Wisen et al.[3] reported that massively obese patients absorbed a fat-rich meal more rapidly and effectively in the proximal intestine during a similar or shorter exposure time. In our study, lipid accumulation was observed in the duodenum of obese individuals, which was accompanied by the increased expression levels of nutrient absorption-related proteins such as CD36 and DGAT2. In recent years, pharmacological inhibitors of lipid absorption have

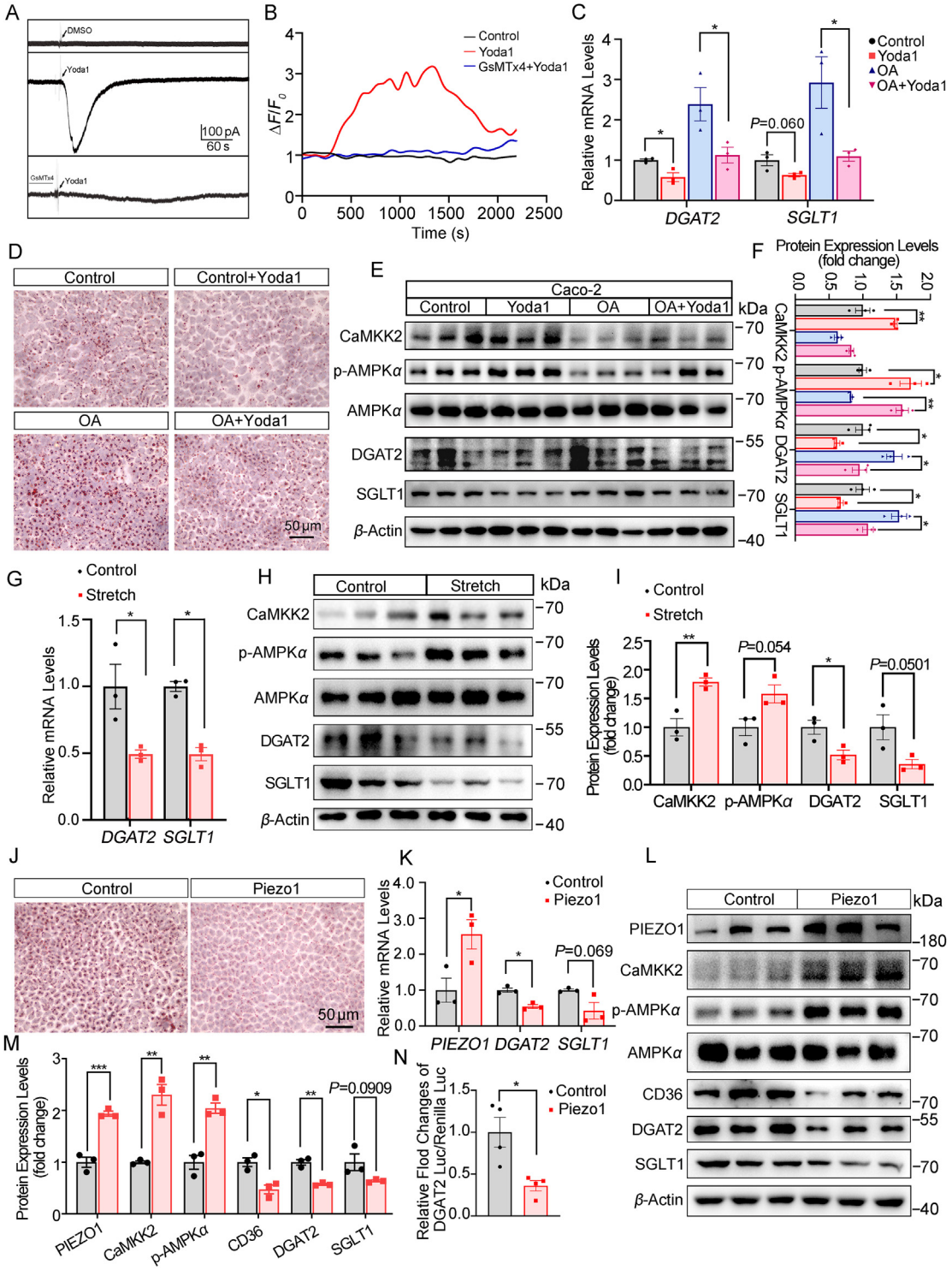

Figure 6 Effects of activating Piezo1 on the lipid metabolism in Caco-2 cells. (A) Whole-cell currents induced by Yoda1 were recorded from Caco-2 cells or pretreated with GsMTx4. (B) The fluorescent intensity ($\Delta F/F_0$) change of intracellular calcium imaging in Caco-2 cells. (C−F) Caco-2 cells treated with Yoda1 and/or OA. (C) The mRNA levels of *DGAT2* and *SGLT1* in Caco-2 cells after treated with Yoda1 and OA. (D) Oil red O staining. (E) Western blot analysis of CaMKK2, p-AMPKα, AMPKα, DGAT2, SGLT1 and β-actin. (F) Quantitative Western blot analysis. (G−I) Caco-2 cells were subjected to mechanical stretch. (G) The mRNA levels of *DGAT2* and *SGLT1* in Caco-2 cells. (H) Representative Western blots for CaMKK2, p-AMPKα, AMPKα, DGAT2, SGLT1 and β-actin. (I) Quantitative Western blot analysis. (J−N) Caco-2 cells were transfected with Piezo1 plasmid. (J) Oil red O staining. (K) The mRNA levels of *PIEZO1*, *DGAT2* and *SGLT1* in Caco-2 cells. (L) Representative Western blots for PIEZO1, CaMKK2, p-AMPKα, AMPKα, CD36, DGAT2, SGLT1 and β-actin. (M) Quantitative Western blot analysis. (N) Overexpression of Piezo1 inhibited Dgat2 promoter activity. Results are presented as the mean ± SEM obtained from three independent experiments. $^*P < 0.05$, $^{**}P < 0.01$, $^{***}P < 0.001$.

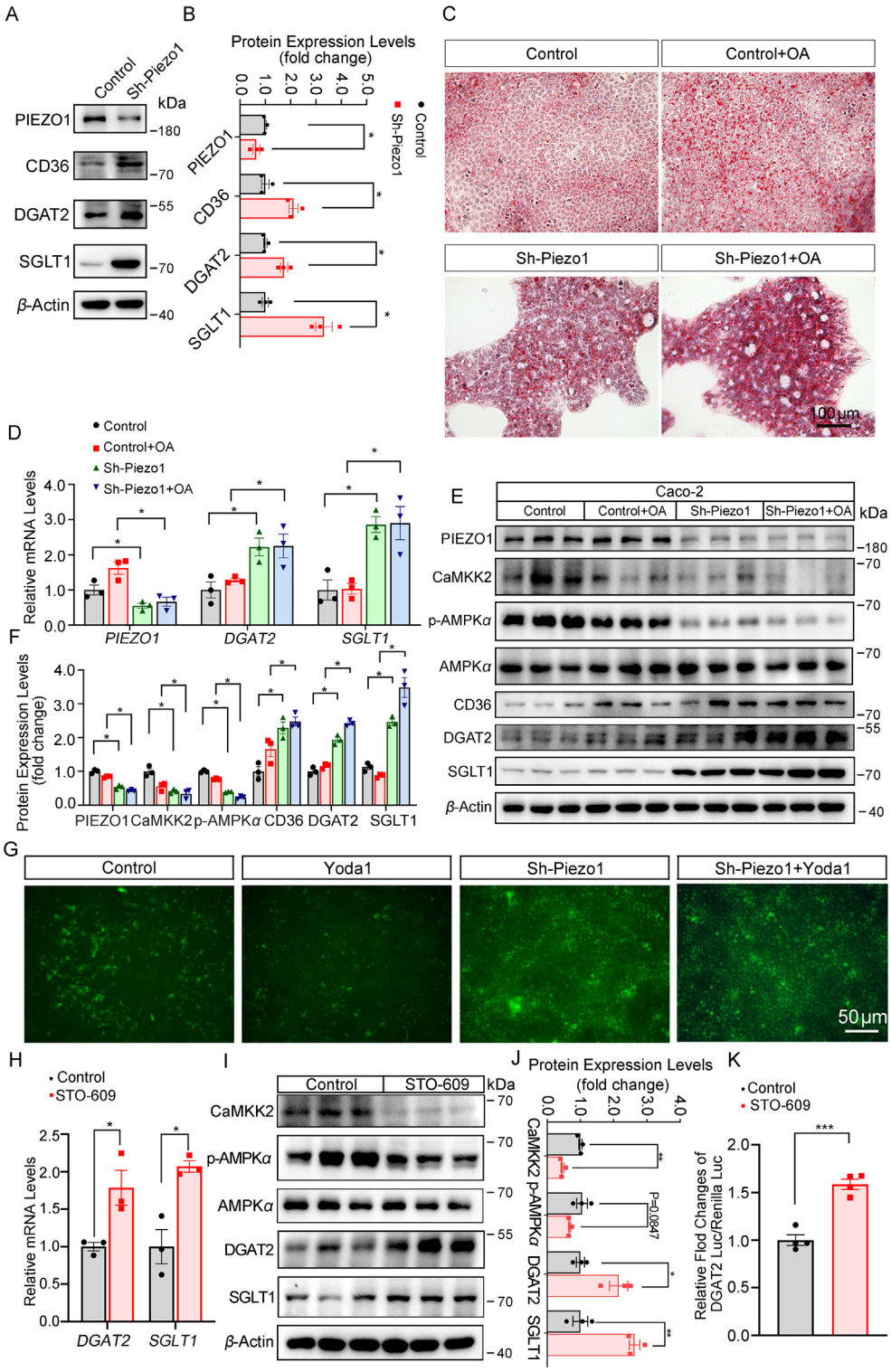

Figure 7 Effects of inhibiting Piezo1 or CaMKK2 on the sugar and lipid metabolism in Caco-2 cells. (A) Stable knockdown of Piezo1 in Caco-2 cells. Representative Western blots for PIEZO1, CD36, DGAT2, SGLT1 and β-actin. (B) Quantitative Western blot analysis. (C) Oil-red O staining of lipid droplets in Caco-2 cells or Piezo1-knockdown Caco-2 cells treated with or without oleic acid (125 μmol/L). (D) The mRNA levels of *PIEZO1*, *DGAT2* and *SGLT1*. (E) Western blot analysis of PIEZO1, CaMKK2, p-AMPKα, AMPKα, CD36, DGAT2, and SGLT1 in Caco-2 cells or Piezo1-knockdown Caco-2 cells treated with or without oleic acid. (F) Quantitative Western blot analysis. (G) Fluorescence imaging of 2-NBDG uptake on Caco-2 cells and Piezo1-knockdown Caco-2 cells. (H−K) Caco-2 cells were treated with STO-609. (H) The mRNA levels of *DGAT2* and *SGLT1* in Caco-2 cells. (I) Representative western blots for CaMKK2, p-AMPKα, AMPKα, DGAT2, SGLT1 and β-actin. (J) Quantitative Western blot analysis. (K) STO-609 stimualted DGAT2 promoter activity. Results are presented as the mean ± SEM obtained from three independent experiments. $^{*}P < 0.05$, $^{**}P < 0.01$, $^{***}P < 0.001$.

been approved for obesity treatment in humans[22,49-52]. Therefore, targeted regulation of nutrient absorption can be an effective intervention in obesity.

After eating, the increase in pressure and motility in the intestines promotes the flow of lymph, leading to a surge in nutrient absorption[53]. It remains unclear whether intestinal epithelial cells sense intestinal distention thus regulate the nutrient absorption. Piezo1 is a mechanosensitive ion channel, which is widely expressed in various tissues including digestive tract and is involved in regulating gut barrier functions and intestinal motility[32,33,54]. In current study, lipid accumulation was observed in the duodenum of obese patients, which was accompanied by down-regulation of Piezo1. We thus hypothesize that Piezo1 may function as a negative regulator for intestinal lipid and glucose absorption. Intestine-specific absence of Piezo1 has limited influence on body weight and glucose metabolism under normal dietary conditions, which consistent to previous reports[33]. However, increased duodenal and hepatic lipid accumulation were exhibited in *Piezo1*^{iKO} mice. Interestingly, *Piezo1*^{iKO} showed no changes in food and water intake, while their duodenal villi became significantly longer than controls. It is reported that enterocytes have two different dynamic storage pools for lipids. Fatty acids absorbed from the intestinal lumen are mainly used for synthesizing TAG, which are then secreted into the lymphatic system in the form of chylomicrons[14]. On the other hand, fatty acids from the circulatory system, specifically from the basolateral side, are primarily utilized for synthesizing phospholipids and undergoing fatty acid oxidation[55]. In our study, absorption-related proteins such as DGAT2, APOB-48 and the transcriptional activators and enzymes involved in fatty acid oxidation including PGC1α, PPARα and ACADL were increased in *Piezo1*^{iKO} mice under NCD. Ramachandran et al.[56] reported that enhanced enterocyte fatty acid oxidation could protect mice from DIO and impaired glycemic control. We speculate that the deletion of Piezo1 in the intestinal tract of mice enhances fatty acid synthesis and chylomicron assembly. However, the increased β-oxidation may effectively manage excessive lipid accumulation, leading to less pronounced lipid accumulation in the blood, intestine, and liver under a normal chow diet (NCD).

When exposed to a high nutrient-rich condition, the *Piezo1*^{iKO} mice exhibited multiple organ lipid deposits, insulin resistance and glucose intolerance. D-Xylose and olive oil gavage assay verified intestinal sugar and lipid absorption were increased in *Piezo1*^{iKO} mice. Key factors related to sugar and lipid metabolism such as SGLT1 and DGAT2 were increased, while transcription factors and enzymes that control fatty acid β-oxidation including PPARα, PGC1α, and ACADL were decreased in *Piezo1*^{iKO} mice under HFD. Excessive lipid accumulation in duodenum and liver may attributed to reduced β-oxidation and stimulated TAG re-synthesis in intestinal epithelial cells. These observations emphasize the vital role of Piezo1 in regulating lipid metabolism and preventing excessive fat absorption. Additionally, obese individuals exhibited a reduction in Piezo1 expression in the duodenum, indicating that the dysfunction of Piezo1-mediated mechanical sensing in intestinal epithelial cells is a crucial mechanism in the development of obesity. The deficiency of Piezo1 may further contribute to increased fat absorption, thus perpetuating multiple organ lipid deposition in obese patients. Yoda1, a Piezo1 agonist, could effectively inhibit SGLT1 and DGAT2 as well as alleviate intestinal absorption of lipids in DIO mice. In Caco-2 cells, knockdown of Piezo1 significantly up-regulated the expression of proteins associated with lipid absorption, resulting in a marked increase in lipid accumulation. Conversely, pharmacological, mechanical and genetic activation of Piezo1 led a notable decrease in the expression of these proteins involved in sugar and lipid absorption. These findings provide new insights into the mechanisms underlying lipid absorption and emphasize the potential therapeutic value of targeting Piezo1 for the treatment of metabolic disorders, particularly obesity.

Piezo1 is a non-selective cationic channel that allows passage of Ca^{2+}. Ca^{2+} binds to its primary intracellular receptor, Calmodulin (CaM), to initiate a diverse array of downstream processes and pathways. Calcium/calmodulin-dependent protein kinase 2 (CaMKK2) is a serine/threonine-protein kinase that belongs to the Ca^{2+}/calmodulin-dependent protein kinase subfamily, which plays critical role in the regulation of metabolic homeostasis[37]. CaMKK2-dependent activation of AMP-activated protein kinase (AMPK) leads to regulation of energy balance, particularly in the brain, liver and adipose[57-59]. Studies have demonstrated that AMPK can regulate the body's glucose and lipid metabolism through proteins such as SGLT1 and DGAT2[60-62]. In current investigation, Piezo1 modulates the expression of DGAT2 and SGLT1 *via* the CaMKK2/AMPKα pathway in the gut.

5. Conclusions

Piezo1 is primarily found in non-excitable cell types and is essential for transducing mechanical forces exerted on the plasma membrane, both externally and internally. Its expression in the intestine has been linked to the regulation of various critical functions, including barrier integrity, mucus secretion, and serotonin synthesis[31,32]. Our study verified the role of Piezo1 in enterocytes inhibits intestinal sugar and lipid absorption, and revealed a previously unexplored mechano-regulation of nutrient absorption in intestinal epithelial cells, which may shed new light on the therapy of obesity and diabetes.

Acknowledgments

This study was supported by grants from the National Natural Science Foundation of China (82170818, 81770794), Guangdong Basic and Applied Basic Research Foundation (2024A1515 010686, China) and the Fundamental Research Funds for the Central Universities (21620423, China). The author would like to thank Prof. Jinghui Guo (The Chinese University of Hong Kong, Shenzhen, China) for providing Piezo1 plasmid and Prof. Baojian Wu (Guangzhou University of Chinese Medicine, Guangzhou, China) for providing Dgat2 luciferase reporter.

Author contributions

Tian Tao: Data curation, Investigation, Writing − original draft, Formal analysis. Qing Shu: Data curation, Investigation, Formal analysis. Yawen Zhao: Formal analysis, Investigation. Wenying Guo: Formal analysis, Investigation. Jinting Wang: Investigation. Yuhao Shi: Investigation. Shiqi Jia: Data curation, Resources. Hening Zhai: Investigation, Resources. Hui Chen: Resources, Writing − review & editing. Cunchuan Wang: Conceptualization, Resources, Supervision. Geyang Xu: Conceptualization, Data curation, Formal analysis, Funding acquisition, Investigation, Methodology, Project administration, Resources, Software, Supervision, Validation, Visualization, Writing − review & editing.

Conflicts of interest

The authors declare no competing interests.

Appendix A. Supporting information

Supporting information to this article can be found online at https://doi.org/10.1016/j.apsb.2024.04.016.

References

1. Malik VS, Willet WC, Hu FB. Nearly a decade on—trends, risk factors and policy implications in global obesity. *Nat Rev Endocrinol* 2020;**16**:615–6.
2. Jin X, Qiu T, Li L, Yu R, Chen X, Li C, et al. Pathophysiology of obesity and its associated diseases. *Acta Pharm Sin B* 2023;**13**:2403–24.
3. Wisén O, Johansson C. Gastrointestinal function in obesity: motility, secretion, and absorption following a liquid test meal. *Metabolism* 1992;**41**:390–5.
4. Goodman BE. Insights into digestion and absorption of major nutrients in humans. *Adv Physiol Educ* 2010;**34**:44–53.
5. Röder PV, Geillinger KE, Zietek TS, Thorens B, Koepsell H, Daniel H. The role of SGLT1 and GLUT2 in intestinal glucose transport and sensing. *PLoS One* 2014;**9**:e89977.
6. Li X, Liu Q, Pan Y, Chen S, Zhao Y, Hu Y. New insights into the role of dietary triglyceride absorption in obesity and metabolic diseases. *Front Pharmacol* 2023;**14**:1097835.
7. Nassir F, Wilson B, Han X, Gross RW, Abumrad NA. CD36 is important for fatty acid and cholesterol uptake by the proximal but not distal intestine. *J Biol Chem* 2007;**282**:19493–501.
8. Milger K, Herrmann T, Becker C, Gotthardt D, Zickwolf J, Ehehalt R, et al. Cellular uptake of fatty acids driven by the ER-localized acyl-CoA synthetase FATP4. *J Cell Sci* 2006;**119**:4678–88.
9. Johnston JM, Rao GA. Intestinal absorption of fat. *Protoplasma* 1967; **63**:40–4.
10. Yang LY, Kuksis A. Apparent convergence (at 2-monoacylglycerol level) of phosphatidic acid and 2-monoacylglycerol pathways of synthesis of chylomicron triacylglycerols. *J Lipid Res* 1991;**32**:1173–86.
11. Kayden HJ, Senior JR, Mattson FH. The monoglyceride pathway of fat absorption in man. *J Clin Invest* 1967;**46**:1695–703.
12. Yen CL, Farese Jr RV. MGAT2, a monoacylglycerol acyltransferase expressed in the small intestine. *J Biol Chem* 2003;**278**:18532–7.
13. Cases S, Smith SJ, Zheng YW, Myers HM, Lear SR, Sande E, et al. Identification of a gene encoding an acyl CoA:diacylglycerol acyltransferase, a key enzyme in triacylglycerol synthesis. *Proc Natl Acad Sci U S A* 1998;**95**:13018–23.
14. Hussain MM. Intestinal lipid absorption and lipoprotein formation. *Curr Opin Lipidol* 2014;**25**:200–6.
15. Ko CW, Qu J, Black DD, Tso P. Regulation of intestinal lipid metabolism: current concepts and relevance to disease. *Nat Rev Gastroenterol Hepatol* 2020;**17**:169–83.
16. Drover VA, Ajmal M, Nassir F, Davidson NO, Nauli AM, Sahoo D, et al. CD36 deficiency impairs intestinal lipid secretion and clearance of chylomicrons from the blood. *J Clin Invest* 2005;**115**:1290–7.
17. Chen HC, Ladha Z, Smith SJ, Farese Jr RV. Analysis of energy expenditure at different ambient temperatures in mice lacking DGAT1. *Am J Physiol Endocrinol Metab* 2003;**284**:E213–8.
18. Stone SJ, Myers HM, Watkins SM, Brown BE, Feingold KR, Elias PM, et al. Lipopenia and skin barrier abnormalities in DGAT2-deficient mice. *J Biol Chem* 2004;**279**:11767–76.
19. Nelson DW, Gao Y, Yen MI, Yen CL. Intestine-specific deletion of acyl-CoA:monoacylglycerol acyltransferase (MGAT) 2 protects mice from diet-induced obesity and glucose intolerance. *J Biol Chem* 2014; **289**:17338–49.
20. Hogue JC, Lamarche B, Tremblay AJ, Bergeron J, Gagné C, Couture P. Evidence of increased secretion of apolipoprotein B-48-containing lipoproteins in subjects with type 2 diabetes. *J Lipid Res* 2007;**48**:1336–42.
21. Musso G, Gambino R, Cassader M, Paschetta E. Efficacy and safety of dual SGLT 1/2 inhibitor sotagliflozin in type 1 diabetes: meta-analysis of randomised controlled trials. *BMJ* 2019;**365**:l1328.
22. Rieg T, Vallon V. Development of SGLT1 and SGLT2 inhibitors. *Diabetologia* 2018;**61**:2079–86.
23. Kim SW, Ehrman J, Ahn MR, Kondo J, Lopez AAM, Oh YS, et al. Shear stress induces noncanonical autophagy in intestinal epithelial monolayers. *Mol Biol Cell* 2017;**28**:3043–56.
24. Coste B, Mathur J, Schmidt M, Earley TJ, Ranade S, Petrus MJ, et al. Piezo1 and Piezo2 are essential components of distinct mechanically activated cation channels. *Science* 2010;**330**:55–60.
25. Song S, Zhang H, Wang X, Chen W, Cao W, Zhang Z, et al. The role of mechanosensitive Piezo1 channel in diseases. *Prog Biophys Mol Biol* 2022;**172**:39–49.
26. Zhong M, Wu W, Kang H, Hong Z, Xiong S, Gao X, et al. Alveolar stretch activation of endothelial Piezo1 protects adherens junctions and lung vascular barrier. *Am J Respir Cell Mol Biol* 2020;**62**:168–77.
27. Wang S, Chennupati R, Kaur H, Iring A, Wettschureck N, Offermanns S. Endothelial cation channel PIEZO1 controls blood pressure by mediating flow-induced ATP release. *J Clin Invest* 2016;**126**:4527–36.
28. Li J, Hou B, Tumova S, Muraki K, Bruns A, Ludlow MJ, et al. Piezo1 integration of vascular architecture with physiological force. *Nature* 2014;**515**:279–82.
29. Faucherre A, Kissa K, Nargeot J, Mangoni ME, Jopling C. Piezo1 plays a role in erythrocyte volume homeostasis. *Haematologica* 2014;**99**:70–5.
30. Li X, Hu J, Zhao X, Li J, Chen Y. Piezo channels in the urinary system. *Exp Mol Med* 2022;**54**:697–710.
31. Zhang J, Zhou Y, Huang T, Wu F, Liu L, Kwan JSH, et al. PIEZO1 functions as a potential oncogene by promoting cell proliferation and migration in gastric carcinogenesis. *Mol Carcinog* 2018;**57**: 1144–55.
32. Jiang Y, Song J, Xu Y, Liu C, Qian W, Bai T, et al. Piezo1 regulates intestinal epithelial function by affecting the tight junction protein claudin-1 *via* the ROCK pathway. *Life Sci* 2021;**275**:119254.
33. Sugisawa E, Takayama Y, Takemura N, Kondo T, Hatakeyama S, Kumagai Y, et al. RNA sensing by gut Piezo1 is essential for systemic serotonin synthesis. *Cell* 2020;**182**. 609-24.e21.
34. Lin Y, Liu R, Huang Y, Yang Z, Xian J, Huang J, et al. Reactivation of PPARα alleviates myocardial lipid accumulation and cardiac dysfunction by improving fatty acid β-oxidation in Dsg2-deficient arrhythmogenic cardiomyopathy. *Acta Pharm Sin B* 2023;**13**:192–203.
35. Kumar A, Hecht C, Priyamvada S, Anbazhagan AN, Alakkam A, Borthakur A, et al. Probiotic *Bifidobacterium* species stimulate human *SLC26A3* gene function and expression in intestinal epithelial cells. *Am J Physiol Cell Physiol* 2014;**307**:C1084–92.
36. Zhang H, Li Q, Teng Y, Lin Y, Li S, Qin T, et al. Interleukin-27 decreases ghrelin production through signal transducer and activator of transcription 3-mechanistic target of rapamycin signaling. *Acta Pharm Sin B* 2020;**10**:837–49.
37. Racioppi L, Means AR. Calcium/calmodulin-dependent protein kinase kinase 2: roles in signaling and pathophysiology. *J Biol Chem* 2012; **287**:31658–65.
38. Marcelo KL, Means AR, York B. The Ca^{2+}/Calmodulin/CaMKK2 axis: nature's metabolic CaMshaft. *Trends Endocrinol Metab* 2016;**27**: 706–18.
39. Pang G, Xie J, Chen Q, Hu Z. Energy intake, metabolic homeostasis, and human health. *Food Sci Hum Well* 2014;**3**:89–103.
40. Hellström PM, Grybäck P, Jacobsson H. The physiology of gastric emptying. *Best Pract Res Clin Anaesthesiol* 2006;**20**:397–407.
41. Evenepoel P. Alteration in digestion and absorption of nutrients during profound acid suppression. *Best Pract Res Clin Gastroenterol* 2001; **15**:539–51.
42. Bäckhed F, Ding H, Wang T, Hooper LV, Koh GY, Nagy A, et al. The gut microbiota as an environmental factor that regulates fat storage. *Proc Natl Acad Sci U S A* 2004;**101**:15718–23.

43. Westergaard H, Dietschy JM. The mechanism whereby bile acid micelles increase the rate of fatty acid and cholesterol uptake into the intestinal mucosal cell. *J Clin Invest* 1976;**58**:97−108.
44. Kiela PR, Ghishan FK. Physiology of intestinal absorption and secretion. *Best Pract Res Clin Gastroenterol* 2016;**30**:145−59.
45. McCauley HA. Enteroendocrine regulation of nutrient absorption. *J Nutr* 2020;**150**:10−21.
46. Mourad FH, Saadé NE. Neural regulation of intestinal nutrient absorption. *Prog Neurobiol* 2011;**95**:149−62.
47. Nguyen NQ, Debreceni TL, Bambrick JE, Chia B, Wishart J, Deane AM, et al. Accelerated intestinal glucose absorption in morbidly obese humans: relationship to glucose transporters, incretin hormones, and glycemia. *J Clin Endocrinol Metab* 2015;**100**:968−76.
48. Iqbal J, Hussain MM. Intestinal lipid absorption. *Am J Physiol Endocrinol Metab* 2009;**296**:E1183−94.
49. Bilheimer DW, Grundy SM, Brown MS, Goldstein JL. Mevinolin and colestipol stimulate receptor-mediated clearance of low density lipoprotein from plasma in familial hypercholesterolemia heterozygotes. *Proc Natl Acad Sci U S A* 1983;**80**:4124−8.
50. Zambre VP, Khamkar SM, Gavhane DD, Khedkar SC, Chavan MR, Pandey MM, et al. Patent landscape for discovery of promising acyltransferase DGAT and MGAT inhibitors. *Expert Opin Ther Pat* 2020;**30**:873−96.
51. Mansor LS, Sousa Fialho MDL, Yea G, Coumans WA, West JA, Kerr M, et al. Inhibition of sarcolemmal FAT/CD36 by sulfo-*N*-succinimidyl oleate rapidly corrects metabolism and restores function in the diabetic heart following hypoxia/reoxygenation. *Cardiovasc Res* 2017;**113**:737−48.
52. Bell DA, Hooper AJ, Burnett JR. Mipomersen, an antisense apolipoprotein B synthesis inhibitor. *Expet Opin Invest Drugs* 2011;**20**:265−72.
53. Tso P, Pitts V, Granger DN. Role of lymph flow in intestinal chylomicron transport. *Am J Physiol* 1985;**249**:G21−8.
54. Xu Y, Xiong Y, Liu Y, Li G, Bai T, Zheng G, et al. Activation of goblet cell Piezo1 alleviates mucus barrier damage in mice exposed to WAS by inhibiting H3K9me3 modification. *Cell Biosci* 2023;**13**:7.
55. Mansbach CM 2nd, Dowell RF. Uptake and metabolism of circulating fatty acids by rat intestine. *Am J Physiol* 1992;**263**:G927−33.
56. Ramachandran D, Clara R, Fedele S, Michel L, Burkard J, Kaufman S, et al. Enhancing enterocyte fatty acid oxidation in mice affects glycemic control depending on dietary fat. *Sci Rep* 2018;**8**:10818.
57. Muraleedharan R, Dasgupta B. AMPK in the brain: its roles in glucose and neural metabolism. *FEBS J* 2022;**289**:2247−62.
58. Anderson KA, Lin F, Ribar TJ, Stevens RD, Muehlbauer MJ, Newgard CB, et al. Deletion of CaMKK2 from the liver lowers blood glucose and improves whole-body glucose tolerance in the mouse. *Mol Endocrinol* 2012;**26**:281−91.
59. Lin F, Ribar TJ, Means AR. The Ca^{2+}/calmodulin-dependent protein kinase kinase, CaMKK2, inhibits preadipocyte differentiation. *Endocrinology* 2011;**152**:3668−79.
60. O'Neill HM, Holloway GP, Steinberg GR. AMPK regulation of fatty acid metabolism and mitochondrial biogenesis: implications for obesity. *Mol Cell Endocrinol* 2013;**366**:135−51.
61. Li B, Fu L, Abe C, Nectoux AM, Yamamoto A, Matsui T. Theaflavins inhibit glucose transport across Caco-2 cells through the down-regulation of the Ca^{2+}/AMP-activated protein kinase-mediated glucose transporter SGLT1. *J Funct Foods* 2020;**75**:104273.
62. Assifi MM, Suchankova G, Constant S, Prentki M, Saha AK, Ruderman NB. AMP-activated protein kinase and coordination of hepatic fatty acid metabolism of starved/carbohydrate-refed rats. *Am J Physiol Endocrinol Metab* 2005;**289**:E794−800.